Songklanakarin J. Sci. Technol.
43 (2), 588-595, Mar. - Apr. 2021

http://www.sjst.psu.ac.th

Original Article

Optimization of quantum dots for solar cell applications

Lekshmi Gangadhar and P. K Praseetha*

Department of Nanotechnology, Noorul Islam Centre for Higher Education, Kumaracoil, Kanya Kumara, Tamil Nadu, 629180 India

Received: 17 September 2018; Revised: 3 December 2019; Accepted: 14 April 2020

Abstract

The quantum dots-sensitized solar cells (QDSSC) provide an alternative concept to present day photovoltaic devices. Cadmium sulfide/Zinc sulfide-sensitized solar cells have been synthesized by chemical bath deposition, based on an aqueous medium involving cadmium sulphate, zinc acetate, thiourea and ammonium hydroxide. To improve the luminescence efficiency and photo stability of the quantum dots (QDs), coating the quantum dots with another wide bandgap semiconductor is a usual procedure. In particular, for CdS quantum dots, the particles were covered with ZnS to establish a core/shell system. This CdS/ZnS quantum dots are assembled onto nanoporous TiO_2 films for quantum dots-sensitized solar cell applications. Physical and chemical properties of the formed nanoparticles were analyzed using field emission scanning electron microscope (FE-SEM), ultraviolet-visible light (UV-VIS) spectrometer, Fourier transform infrared spectroscopy (FTIR) and X-ray diffraction (XRD). An efficiency as high as 1.80% for the CdS/ZnS quantum dots-sensitized solar cells was achieved using the present method.

Keywords: cadmium sulfide, zinc sulfide, quantum dots, core/shell, solar cells

1. Introduction

Nanosized inorganic semiconducting materials have been generating extensive interest in recent years owing to their structure, chemical and physical properties, which are different from those of the bulk materials. Therefore, much effort has been made to control the size, morphology and polycrystallinity of the nanocrystals with a view to tune their physical properties. Quantum dots are small particles of a semiconductor with typical dimensions from 1nm to 10nm. Just as in an atom, the energy levels of quantum dots are quantized due to the confinement of electrons. Quantum dots have unique spectral properties such as broad absorption, and narrow emission with wavelength dependent on the size. An important property of quantum dots is their ability to tune the band gap and therefore to control the light absorbance and emission frequencies. In this way the electrical and optical properties can be adjusted according to the targeted purpose.

*Corresponding author
Email address: crkpkp@gmail.com

Quantum dots absorb photons of light and then emit longer wavelengths of photons for a period of time. The high controllability of the size of quantum dots gives a way to precisely control the wavelength of the emitted photons. That means the colour of the light emitted from the Quantum dot can actually be manipulated without significant cost, with the use of nanotechnology. Following these procedures, a full range of quantum dots can be manufactured each with a distinct emission spectrum. Quantum dots confine electrons or holes in all the three dimensions and allow no free propagation. In quantum dots the energy levels become discrete and the energy is larger than in bulk material.

The electrons exist in different energy levels as in bulk semiconductors. In these materials there is a forbidden range of energies known as the bandgap. The lower energy level is called the valence band and the higher energy level above the energy gap is called the conduction band. On absorbing some sort of stimulus such as light or heat, an electron can rise to the conduction band from the valence band. This leaves behind a hole in the valence band, and the hole and the electron together are called an exciton. The average difference between the hole and the electron in exciton is called the excited Bohr radius. When the size of the

semiconductor falls below the Bohr radius the semiconductor is called a quantum dot. The exciton has a limited life time and the electron will come back to the valence band and recombine with the hole. The recombination process is usually a radiator process that includes photon release or fluorescence. The absorption and fluorescence process can be measured, and the confinement in the quantum dot arises from the electrostatic potentials usually generated by external electrons from doping or added impurities.

The smaller the size of the crystal, the lesser the band gap, the greater the energy between the highest valence band and lowest conduction band becomes. Therefore more energy is needed to excite the dots and so more energy is released when the crystal returns to its restored states. This requires higher frequencies of light for excitation of the dots as the crystal size goes smaller resulting in an equivalent shift from high to low wavelength in the light emitted. As the nanomaterial becomes larger, the energy gap becomes smaller and the quantum dot changes its colour from violet towards red. In addition to tuning of size, the main advantage with quantum dots is that because of the good control of their size, there is a way to precisely control the conductive properties over the conductive material.

Quantum dots are made largely from the elements in the second and sixth group of the periodic system – Cadmium Chalcogenides (CdS, CdSe, and CdTe), Zinc (ZnSe, ZnS, ZnTe) and third and fifth group, Phosphides and Indium Arsenides (Biswas, Hossain, & Takahashi, 2008). Quantum dots can be engineered to fluoresce in different wavelengths based on their physical dimensions. Sulfides are wide bandgap II-VI semiconductor materials, and have been studied extensively due to their wide applications in the fields of solar cells, light-emitting devices and optical recording materials (Dethlefsen & Dossing, 2011). Solar cells have attracted significant attention due to their promising applications in energy generation. The photovoltaic (PV) effect was observed by Becquerel, who reported a current flow between two silver electrodes in an electrolyte media upon light exposure. Since the pioneering report by O'Regan and Grätzel, dye-sensitized solar cells have been investigated extensively all over the world (Gratzel & O'Regan, 1991). The quantum dot sensitized solar cell has received wide attention recently because it has several advantages over dye sensitized cells, such as tunable energy gaps, high absorption coefficients and generation of multiple electron-hole pairs with high energy excitation. The TiO_2 nanoparticle based photoelectrode showed considerable power conversion efficiency over a large surface area (Liao, Lei, Kuang & Su, 2011). It has been accepted that the value of power conversion efficiency of photo electrodes strongly depends on the morphology and structure of TiO_2. In order to increase the photovoltaic performance, because of their excellent electron transport and light scattering ability, nanostructures such as nanorods, nanowires or nanotubes have been studied as photoelectrode materials for sensitized solar cells.

The quantum dot sensitizing of a solar cell is based on the bandgap alteration due to the quantum confinement effect. Much research has been done on the fabrication of quantum dot sensitized solar cells, in which quantum dots are embedded in mesoporous TiO_2 structure by chemical bath deposition (Malgras, Nattestad, Kim, Dou & Yamauchi, 2017). The surface properties of quantum dots can be modified in order to increase the photo stability of the electrodes (Klein, Roth, Lim, Alivisatos, & McEuen, 1997). CdS has shown much prospect as a sensitizer. High luminescence efficiency and stability have been achieved for core-shell nanoparticles (Steckel, Zimmer, Coe-Sullivan, Stott, Bulovic & Bawendi, 2004). Studies on solar cells aim to achieve high energy conversion efficiencies, mass production at a low cost, and improved energy storage. Photovoltaic solar cells fall into several categories, depending on the material type, the highest achievable conversion efficiency and the cost of photovoltaic energy. Various generations of solar cells are given in Figure 1.

Generally, DSCs consist of a transparent conductive oxide (TCO) electrode coated with mesoporous TiO_2 film which is sensitized with dyes, a platinum coated counter electrode, and an electrolyte containing an iodide/tri-iodide redox couple filled between these two electrodes (Kumar, Barman & Singh 2014; Prasad & Elumalai 2011). The absorption spectrum of sensitizer plays an important role in achieving high energy conversion efficiency. The application of semiconductor quantum dots as sensitizers has some advantages in sensitized solar cells (Kongkanand, Tvrdy, Takechi, Kuno & Kamat, 2008). The CdS quantum dot particles were covered with ZnS to establish a core/shell system, where the bandgap of the core lies energetically within the bandgap of the shell material, and the photogenerated electrons and holes are mainly confined inside the CdS (Macdonald & Nann, 2011). As the ZnS shell

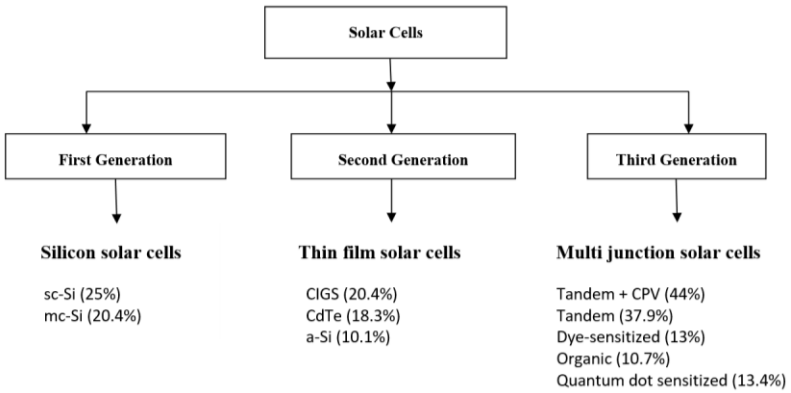

Figure 1. Generations of solar cell

thickness increases, there could be an increased electron–hole pair generation leading to large free-carrier concentration, which in turn results in enhanced nonlinear optical absorption (Grabolle, Ziegler, Merkulov, Nann & Resch-Genger, 2008). In addition, it was found that the optical limiting threshold decreased as the ZnS shell thickness increased (Guo *et al.*, 2012). The bandgap is easily controlled by the size of the quantum dots and thereby the absorption spectrum can be adjusted to match the spectral distribution of sunlight, and the band edge type absorption behavior is most favorable for effective light harvesting (Gratzel, 2005). The surface properties of the quantum dots can be modified in order to increase the photo stability of the electrodes.

A QDSSC is composed of quantum dots adsorbed on nanoporous TiO_2 layer on a fluorine-doped tin oxide (FTO) glass substrate, redox electrolytes and a counter electrode (Kong *et al.*, 2012; Liao, Lei, Chen, Kuang & Su, 2012; Liao, Lei, Kuang & Su, 2011). A unidirectional charge flow with no leakage of electrons at the interfaces is essential for high energy-conversion efficiency. The energy-conversion efficiency is likely to be dependent on the morphology and structure of the quantum dots adsorbed on TiO_2 film (Pavan *et al.*, 2015). TiO_2 films are used as photoanodes to enhance the effective surface area, to absorb more quantum dots and thus to achieve more light absorption and greater efficiency. The high conversion efficiency achieved by the QDSSC may be attributed to its uniquely porous Titania film, quantum dots and the electrolyte. To improve electron transport, we have to provide a large surface area to adsorb the sensitized quantum dots and enhance incident light harvest. QDSSCs were constructed by the application of TNWs and TiO_2 nanoparticles (Fan *et al.*, 2009). TNWs were fabricated by a hydrothermal process. The introduction of TNWs, with a much more open structure, enables the electrolyte to penetrate easily inside the film, increasing the interfacial contact between the nanowires, the quantum dots and the electrolyte. It is expected that the photoelectrical performance of the QDSSC can be further improved.

2. Experimental details

2.1 Preparation of CdS/ZnS quantum dots

The starting materials are Cadmium sulphate as a Cd^{++} ion source and thiourea as an S^{--} ion source. An alkaline solution of ammonia is used to adjust pH of the reaction mixture. Ammonium hydroxide is added drop wise to cadmium sulphate solution at 50°C to adjust pH to 11. Thiourea is added drop wise to this, which results in yellow precipitate of CdS quantum dots. Zinc acetate solution is added to this followed by addition of ammonium hydroxide. Thiourea is added drop wise and results in precipitation of CdS/ZnS quantum dots. Filter the precipitate and wash several times with double distilled water, and dry in an oven at 70°C to collect nanopowder, namely CdS/ZnS quantum dots.

2.2 Preparation of CdS/ZnS quantum dots using leaf extract

Moringa oleifera leaves have sulfur-containing amino acids at high levels. Moringa oleifera extract was prepared by taking 20g of dry Moringa oleifera leaves, which were thoroughly washed and finely crushed and mixed with 50ml of deionized water before boiling the mixture at 80ºC for 15 min. After cooling to room temperature the extract was filtered by Whatman filter paper (Prasad & Elumalai, 2011). The Cd^{++} ion source is Cadmium sulphate and S^{--} ion source is moringa oleifera extract. An alkaline solution of ammonia is used to adjust pH of the reaction mixture. Ammonium hydroxide is added dropwise to cadmium sulphate solution at 50°C to adjust pH to 11. Moringa oleifera leaf extract is added drop wise to this, which results in yellow precipitate of CdS quantum dots. Zinc acetate solution is added to this followed by addition of ammonium hydroxide. Moringa oleifera leaf extract is added drop wise to precipitate CdS/ZnS quantum dots. Filter the precipitate and wash several times with double distilled water and dry in an oven at 70°C to collect nanopowder of CdS/ZnS quantum dots.

2.3 Preparation of TiO_2 nanowires

Take 0.1gram of anatase TiO_2 (Aldrich Chemical, Sigma-Aldrich Corporation, St. Louis, MO, USA) and 40 ml of 10 M NaOH, heated under stirring at 100º C for 5 hours. The mixture is kept in an oven at 200º C for 24 hours. The resultant sample is filtered. The filtrate is taken and 1M HCl is added drop wise under stirring until the pH becomes 7. The precipitate formed is filtered, then washed sequentially with double distilled water and ethanol, several times. The sample is dried in a hot air oven at 70º C for 8 hours, and a fibrous white product is obtained.

2.4 Assembly of the QDSSCs

The QDSSCs are composed of four main components: wide bandgap semiconductor film (TiO_2) crystalline nanoparticles on FTO glass, QDs adsorbed onto these nanoparticles, hole conductor electrolyte which penetrates the nanocrystalline semiconductor network, and a graphite counter electrode. The working electrode used was TiO_2 coated FTO, sensitized with CdS/ZnS quantum dots. Carbon-based materials like graphite, coated on the FTO glass conducting surface by rubbing with a pencil lead, work well as the counter electrode in the QDSSCs. The cell was fabricated with great care in sandwich form by clamping working electrode and counter electrode, so as to take leads from both the electrodes. An effective working area of 0.25 cm^2 was exposed to light source, while all other areas were masked. For the application of quantum dot sensitized solar cell, potassium iodide electrolyte was developed. A solvent consisting of potassium iodide and ethylene glycol was prepared and stored in a dark container. Prior to clamping, one or two drops of freshly prepared electrolyte were placed above the working electrode. It should be ensured that the whole aperture was covered by the electrolyte and the electrodes were tightly held with the help of a crocodile clip. The structure of QDSSCs is shown in Figure 2.

2.5 Working of QDSSCs

QDSSCs are based on a nanostructure of wide bandgap semiconductor material sensitized with QDs. Excitons are generated by the light absorption to QDs when the QDSSC is illuminated by sunlight. If the electron injection

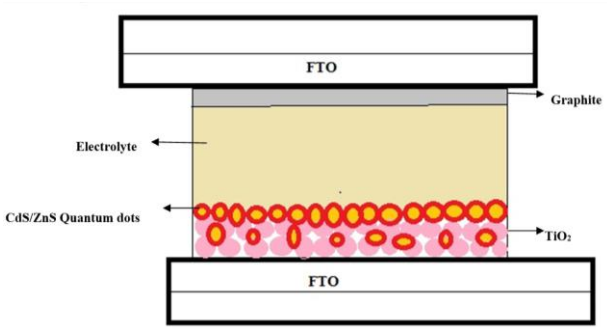

Figure 2. Structure of quantum dot sensitized solar cell

rate is faster than exciton recombination rate then the electrons will transfer to the wide bandgap semiconductor conduction band. By an electrochemical reaction, reduction of the holes left in the QD will happen with the reductant in the electrolyte. The electrons injected to the semiconductor flow to the contact at the anode, through the load and to the cathode where the oxidation reduction takes place in the electrolyte for completion of the circuit. When light with energy greater than or equal to bandgaps of the QDs is illuminating a QDSSC, exciton generation happens in QDs.

$$QD + h\upsilon \rightarrow QD^*$$

$$QD^* \rightarrow QD^+ + e^- (TiO_2)$$

When the single photon energy is larger than the bandgap of the QDs sensitizing the cell, generation of multiple excitons happens. The TiO_2/QDs/electrolyte interface performs the charge separation. The conduction of resultant electrons to the FTO layer by porous TiO_2 and the holes recovery is done by I^-/I_3^- electrolyte. The electron will move to the external circuit through FTO. At the graphite counter electrode, triiodide (I_3^-) is reduced to iodide (I^-) by gaining electrons from the graphite electrode.

$$I_3^- + 2e^- (Graphite) \rightarrow 3I^-$$

I^- is transported through the electrolyte towards the FTO photoelectrode, where it reduces the oxidized QD. The equation helps in understanding the restoration of QDs.

$$2\ QD^+ + 3I^- \rightarrow 2\ QD + I_3^-$$

The energy level position of whole system is the key to charge separation. The QDs excited state should be positioned above the TiO_2 conduction band edge and QDs ground state should be positioned below the chemical potential of redox pair I^-/I_3^- in electrolyte, since then there are energetic driving forces for hole and electron separation. Due to this energy level positioning in the system, the cell is capable of voltage production between its electrodes and the external load.

There is no electric field to force the transport as electric fields are not constant in the electrolyte or in semiconductor nanoparticles. The photo voltage in QDSSC is restricted by the energy difference across the electrolyte redox potential and the conduction band edge of wide bandgap semiconductor. The band diagram of quantum dots is shown in Figure 3. In QDSSC, the charge transfer rate depends on the band alignment of the two materials, which varies dependent on the size of the QD. More of the solar spectrum will be absorbed by a larger QD, but they would not transport the charges generated to the acceptor material effectively. The electron injection rate is dependent on the difference in the wide bandgap semiconductors conduction band and QD conduction band. The solar cell's theoretical efficiency limits depend on the band alignment in the device and on the absorber's optical band gap. For attaining large conversion efficiencies, the difference between the energy of photon at the absorption onset and the photogenerated charge electrical energy should be minimized.

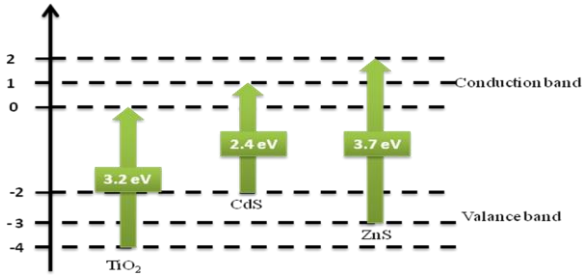

Figure 3. Energy band diagram

3. Results and Discussion

3.1 SEM observations of TiO_2 nanowires and CdS/ZnS quantum dots

SEM pictures revealed that CdS/ZnS quantum dots and TiO_2 nanowires were successfully prepared. SEM pictures shows needle-like self-assembled one-dimensional nanostructures, which may be regarded as TiO_2 nanowires. Figure 4 (a) reveals high yield of the nanowires. The average length of the wires was about 2-4 µm and the average diameter was 40-50 nm. Spherical like structures were observed in CdS/ZnS QDs prepared by chemical bath deposition (CBD), Figure 4 (b) and (c). The crystalline nature of the observed particles is very good. The average diameter of the CdS/ZnS quantum dots prepared by chemical synthesis was about 6-8 nm and the average diameter of CdS/ZnS quantum dots by green synthesis was 7-9 nm.

3.2 TEM observations of CdS/ZnS quantum dots

Transmission electron microscopy has been performed to assess the particle size and the results are presented in Figure 5. TEM image of CdS/ZnS QDs show highly monodisperse nanoparticles with 3-7 nm sizes. It is also clear from the figure that there is no agglomeration of the QDs. The particle size obtained from TEM is in accordance with the size obtained from XRD analysis.

3.3 XRD observations of TiO_2 nanowires and CdS/ZnS quantum dots

The X-ray diffraction (XRD) pattern of TiO_2 nanowire is shown in Figure 6. In case of TiO_2 nanowires, the prominent peaks at d=0.325 and d=0.1628 indicate good crystallinity of the TiO_2 anatase phase. Figure 6 shows the

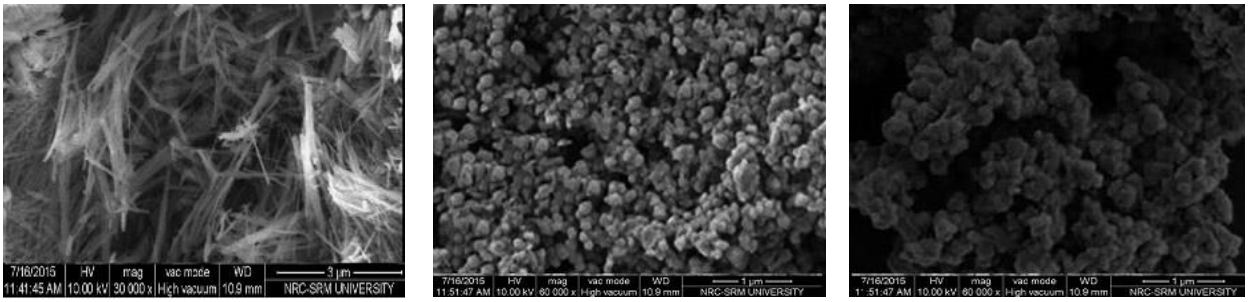

(a) (b) (c)

Figure 4. SEM images of (a) TiO_2 nanowires, (b) CdS/ZnS quantum dots prepared by chemical method, and (c) CdS/ZnS quantum dots prepared by a green method.

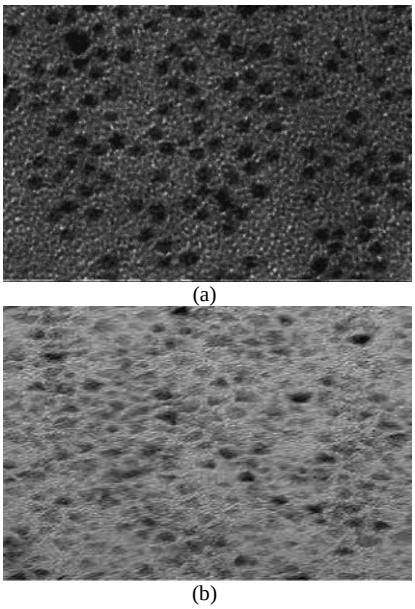

(a) (b)

Figure 5. TEM images of (a) CdS/ZnS quantum dots prepared by chemical method, and (b) CdS/ZnS quantum dots prepared by a green method.

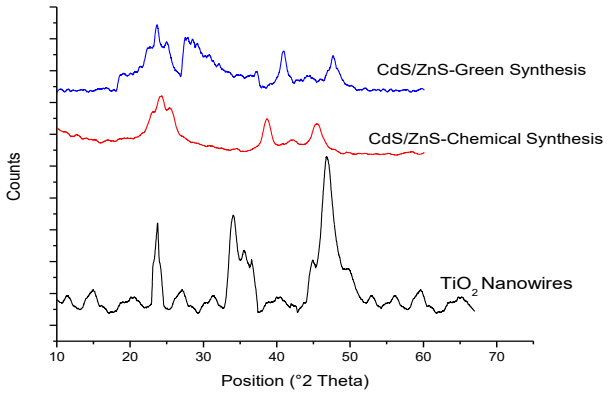

Figure 6. XRD images of TiO_2 nanowires, CdS/ZnS quantum dots prepared by chemical method, and CdS/ZnS quantum dots prepared by a green method.

XRD pattern of the CdS/ZnS QDs deposited by chemical bath deposition (CBD). The most prominent peaks are similar to those for ZnS QDs, i.e. (002) direction along with the other reflections from (200) and (201) planes. These peaks show that ZnS is present at the outer surface in the form of a shell. The average particle size of CdS/ZnS core shell structure was estimated using the Debye Scherrer formula as around 4.2 nm. According to XRD both CdS and ZnS peaks were present in the core shell structure. The presence of high intensity peaks at (2θ = 27.58°) clearly shows that the particle size of CdS/ZnS is very small corresponding to the (002) plane, for CdS/ZnS quantum dots prepared by chemical method. The presence of peaks at 2θ = 25.85°, 42.82°, 47.81° shows that the particle size of CdS/ZnS is very small, around 4.6 nm, for the CdS/ZnS quantum dots prepared by green method.

3.4 UV-Visible Spectroscopy of TiO_2 nanowires and CdS quantum dots

The optical absorption spectrum of TiO_2 nanowires with CdS/ZnS quantum dots is shown in Figure 7. In the absorption spectrum obtained, the peak at 252 nm indicates absorption due to anatase TiO_2. The optical absorption excitonic peak of CdS/ZnS quantum dots is shifted to a lower wavelength relative to that of bulk (~530 nm) crystals. This continuous blue shift shows that quantum confinement occurred in the prepared quantum dots. The absorption edge of the core/shell structure lies between CdS and ZnS quantum dots because surface to volume ratio in core/shell is more than that for CdS but less than that for ZnS.

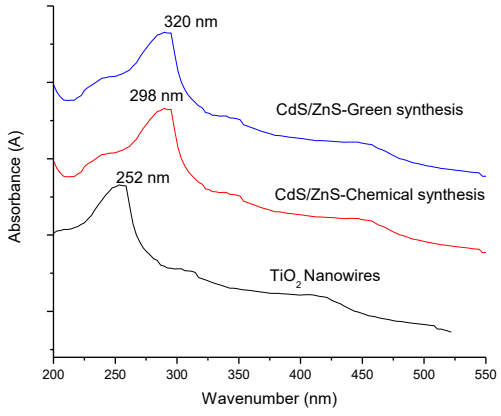

Figure 7. UV-Visible images of TiO_2 nanowires, CdS/ZnS quantum dots prepared by chemical method and CdS/ZnS quantum dots prepared by a green method.

3.5 FTIR of TiO_2 nanowires and CdS/ZnS quantum dots

The relative IR absorbance significantly depends on short range environment of oxygen coordination around cations in the lattice, crystal geometry, and oxidation state of its cations. A typical IR spectrum of the sample was recorded on a NaCl crystal and is shown in Figure 8. TiO_2 - anatase forms nanowires having characteristic peaks at 638, 513 and 397 cm^{-1} that were observed in the FTIR spectrum, Figure 8 (a).The prominent peak from 404 cm^{-1} is a specific characteristic of TiO_2 in anatase form. In Figure 8 (b) a broad absorption band around 3400 cm^{-1} is assigned to O-H vibrations of absorbed H_2O. The absorption band present at 644 cm^{-1} corresponds to Cd-S stretching. The band around 1500 cm^{-1} is due to NH_2 bending. The band near 2353 cm^{-1} can be attributed to C=O residue, probably due to atmospheric CO_2. These results show how effectively ZnS covers the CdS core.

3.6 Photocurrent- voltage (I-V) characteristics QDSSCs

The I-V characteristics of quantum dot sensitized solar cell (FTO/TiO_2/CdS/ZnS QDs/Graphite/FTO) were measured using a solar simulator and the results are shown in Figure 9 (a,b,c). The photocurrent is defined as the current produced under light irradiation due to generation of free charge carriers by absorption of photons within the depletion layer. The efficiency of a solar cell under illumination and non-illumination conditions (with light (wl) and without light (wol)) is also calculated.

The efficiency of the TiO_2 nanowires alone in solar cell is due to photocatalytic activity. For improvement of performance in CdS quantum dots sensitized TiO_2 solar cells and for enhancing the electron diffusion length, the surfaces of the CdS QDs were coated with ZnS, which improved efficiency. The photo conversion efficiency of FTO/TiO_2/ CdS/ZnS QDs/Graphite/FTO solar cell (green) is higher than that of FTO/TiO_2/CdS/ZnS QDs/Graphite/FTO solar cell (chemical). Core/shell semiconductor CdS/ZnS nanocrystals that were synthesized are safe, environmentally friendly, and low-cost. Comparison of efficiency with various QDSSCs is shown in Table 1.

4. Conclusions

CdS/ZnS nanoparticles with core-shell structure were successfully synthesized through aqueous chemical route, and their structural as well as optical properties were investigated by XRD, UV-Vis spectroscopy, FTIR, SEM and TEM. XRD results indicated that a lower synthesis temperature resulted in smaller grain size, and the particle sizes of CdS/ZnS quantum dots as determined from XRD and TEM image are in a good agreement. The UV-Visible spectra show a large blue shift, and this size dependent blue shift of absorption edge is attributed to the quantum size effect. Core/shell semiconductor nanocrystals that were prepared by this method are low-cost, safe and environmentally friendly. The crystallization quality of the CdS/ZnS quantum dots was

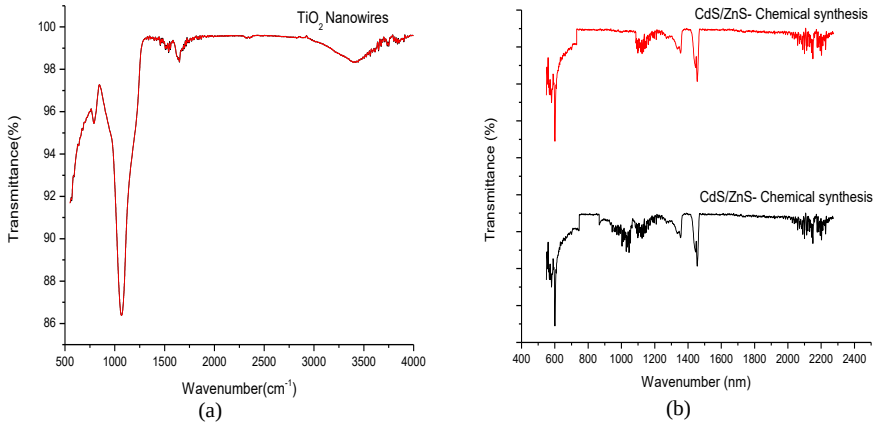

Figure 8. FTIR spectra of (a) TiO_2 nanowires, (b) CdS/ZnS quantum dots prepared by chemical method, and CdS/ZnS quantum dots prepared by a green method.

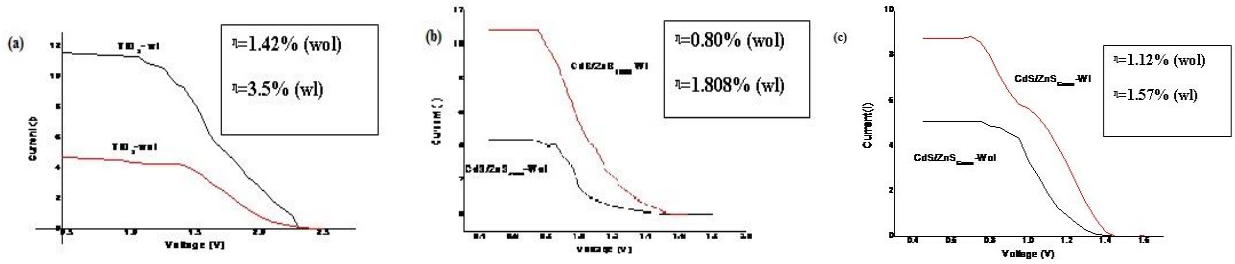

Figure 9. I-V characteristics of (a) TiO_2 nanowires, (b) solar cell with CdS/ZnS quantum dots prepared by chemical method, and (c) solar cell with CdS/ZnS quantum dots prepared by a green method; with light (wl) and without light (wol).

Table 1. Comparison of efficiency with other QDSSCs

No	Types of QDSSCs	Photo conversion efficiency
1.	CdSe	2.1%
2.	CdS/CdSe	4.92%
3.	Mn-doped $CuInS_2$	5.38%
4.	CuInSe	8.1%
5.	CdSexTe1−x	8.55%
6.	Zn-Cu-In-Se	11.6%
7.	PbS/CdS	4.2%
8.	$CuInS_2$/ZnS	7.04%
9.	CdTe/CdSe	6.76%
10.	ZnTe/CdSe	6.82%
11.	CdTe/CdS/CdS	6.32%
12.	CdS/CdSe	5.32%
13.	CdS	0.33%
14.	CdS/ZnS	0.68%
15.	CdS/ZnS(Present work)	1.808%

improved by annealing. By thickness optimization of the TiO_2 electrode, the conversion efficiency is expected to improve further, which is well suited for harvesting more light energy in solar cell applications. The performance optimization of the photoanode is attained by a scattering layer addition and with ZnS layer passivation. Carbon-based materials like graphite, coated on the FTO glass conducting surface by rubbing with a pencil lead, work well as counter electrode in the QDSC. Graphite is a promising substitute of Pt counter electrode due to low cost, environmental friendliness, large surface area, good catalytic activity, better thermal stability, improved electrical conductivity, excellent corrosion resistance with iodine and poly sulfide electrolyte, and high reactivity for tri-iodide reduction. The TiO_2 layer sensitized with QDs and standard electrolytes was explored in the present study in pursuit of higher efficiencies. Absorbing sunlight from the appropriate portion of the solar spectrum and tuning the bandgap of the semiconductor by tuning the size of the quantum dots allow optimizing the performance of the devices. If the performance of the devices is optimized, these low-cost, high-throughput devices could make a huge impact in the energy conversion industry across the globe.

Acknowledgements

We acknowledge all the staff of nanotechnology department laboratory at Noorul Islam University. We extend our gratitude to Dr. P Venugopalan for dedicated discussions and help in the laboratory work.

References

Biswas, S., Hossain, M. F., & Takahashi, T. (2008). Fabrication of Gratzel solar cell with TiO_2/CdS bilayered photoelectrode. *Thin Solid Films*, *517*(3), 1284-1288.

Dethlefsen, J. R., & Døssing, A. (2011). Preparation of a ZnS shell on CdSe quantum dots using a single-molecular ZnS precursor. *Nano Letters*, *11*(5), 1964-1969.

Fan, S. Q., Kim, D., Kim, J. J., Jung, D. W., Kang, S. O., & Ko, J. (2009). Highly efficient CdSe quantum-dot-sensitized TiO_2 photoelectrodes for solar cell applications. *Electrochemistry Communications*, *11*(6), 1337-1339.

Grabolle, M., Ziegler, J., Merkulov, A., Nann, T., & Resch Genger, U. (2008). Stability and fluorescence quantum yield of CdSe–ZnS quantum dots—influence of the thickness of the ZnS shell. *Annals of the New York Academy of Sciences*, *1130*(1), 235-241.

Gratzel, M. (2005). Solar energy conversion by dye-sensitized photovoltaic cells. *Inorganic Chemistry*, *44*(20), 6841-6851.

Gratzel, M., & O'Regan, B. (1991). A low-cost, high-efficiency solar cell based on dye-sensitized colloidal TiO_2 films. *Nature*, *353*(6346), 737-740.

Guo, W., Xu, C., Wang, X., Wang, S., Pan, C., Lin, C., & Wang, Z. L. (2012). Rectangular bunched rutile TiO_2 nanorod arrays grown on carbon fiber for dye-sensitized solar cells. *Journal of the American Chemical Society*, *134*(9), 4437-4441.

Klein, D. L., Roth, R., Lim, A. K., Alivisatos, A. P., & McEuen, P. L. (1997). A single-electron transistor made from a cadmium selenide nanocrystal. *Nature*, *389*(6652), 699.

Kong, E. H., Chang, Y. J., Park, Y. C., Yoon, Y. H., Park, H. J., & Jang, H. M. (2012). Sea urchin TiO_2–nanoparticle hybrid composite photoelectrodes for CdS/CdSe/ZnS quantum-dot-sensitized solar cells. *Physical Chemistry Chemical Physics*, *14*(13), 4620-4625.

Kongkanand, A., Tvrdy, K., Takechi, K., Kuno, M., & Kamat, P. V. (2008). Quantum dot solar cells. Tuning photoresponse through size and shape control of CdSe− TiO_2 architecture. *Journal of the American Chemical Society*, *130*(12), 4007-4015.

Kumar, H., Barman, P. B., & Singh, R. R. (2014). Development of CdS, ZnS quantum dots and their core/shell structures by wet chemical method. *International Journal of Scientific and Engineering Research*.

Liao, J. Y., Lei, B. X., Chen, H. Y., Kuang, D. B., & Su, C. Y. (2012). Oriented hierarchical single crystalline anatase TiO_2 nanowire arrays on Ti-foil substrate for efficient flexible dye-sensitized solar cells. *Energy and Environmental Science*, *5*(2), 5750-5757.

Liao, J. Y., Lei, B. X., Kuang, D. B., & Su, C. Y. (2011). Tri-functional hierarchical TiO_2 spheres consisting of anatase nanorods and nanoparticles for high efficiency dye-sensitized solar cells. *Energy and Environmental Science*, *4*(10), 4079-4085.

Macdonald, T. J., & Nann, T. (2011). Quantum dot sensitized photoelectrodes. *Nanomaterials*, *1*(1), 79-88.

Malgras, V., Nattestad, A., Kim, J. H., Dou, S. X., & Yamauchi, Y. (2017). Understanding chemically processed solar cells based on quantum dots. *Science and Technology of Advanced Materials*, *18*(1), 334-350.

Pavan, M., Rühle, S., Ginsburg, A., Keller, D. A., Barad, H. N., Sberna, P. M., & Fortunato, E. (2015). TiO_2/Cu_2O all-oxide heterojunction solar cells produced by spray pyrolysis. *Solar Energy Materials and Solar Cells*, *132*, 549-556.

Prasad, T. N. V. K. V., & Elumalai, E. K. (2011). Biofabrication of Ag nanoparticles using *Moringa oleifera* leaf extract and their antimicrobial activity. *Asian Pacific Journal of Tropical Biomedicine*, *1*(6), 439-442.

Steckel, J. S., Zimmer, J. P., Coe Sullivan, S., Stott, N. E., Bulović, V., & Bawendi, M. G. (2004). Blue luminescence from (CdS) ZnS core–shell nanocrystals. *Angewandte Chemie International Edition*, *43*(16), 2154-2158.